Gut Microbiota Diversity across Ethnicities in the United States

Authors:

Andrew W. Brooks[1,2], Sambhawa Priya[3,4,5], Ran Blekhman[3,4], Seth R. Bordenstein[1,2,6,7*]

Affiliations:

[1] Vanderbilt Genetics Institute, Vanderbilt University, Nashville, TN, USA.

[2] Department of Biological Sciences, Vanderbilt University, Nashville, TN, USA

[3]Department of Genetics, Cell Biology, and Development, University of Minnesota, Minneapolis, MN, USA

[4]Department of Ecology, Evolution, and Behavior, University of Minnesota, Minneapolis, MN, USA

[5] Bioinformatics and Computational Biology Program, University of Minnesota, Minneapolis, MN, USA

[6] Department of Pathology, Microbiology, and Immunology, Vanderbilt University, Nashville, TN, USA.

[7]Vanderbilt Institute for Infection, Immunology and Inflammation, Vanderbilt University, Nashville, TN, USA.

[*] Corresponding author. E-mail: s.bordenstein@vanderbilt.edu (S.R.B)

Abbreviations:

AGP – American Gut Project

ANOSIM – Analysis of Similarity

AUC – Area Under the Curve

BMI – Body Mass Index

F_{ST} – Fixation Index

GWAS - Genome-Wide Association Studies

HMP – Human Microbiome Project

MAF - Minor Allele Frequency

OTU – Operational Taxonomic Unit

PERMANOVA - Permutational Multivariate Analysis of Variance

RF – Random Forest

ROC – Receiver Operating Characteristic

SMOTE – Synthetic Minority Over-sampling Technique

Abstract:

Composed of hundreds of microbial species, the composition of the human gut microbiota can vary with chronic diseases underlying health disparities that disproportionally affect ethnic minorities. However, the influence of ethnicity on the gut microbiota remains largely unexplored and lacks reproducible generalizations across studies. By distilling associations between ethnicity and gut microbiota variation in two American datasets including 1,673 individuals, we report 12 microbial genera and families that reproducibly vary by ethnicity. Interestingly, a majority of these microbial taxa, including the most heritable bacterial family, Christensenellaceae, overlap with genetically-associated lineages and form co-occurring clusters of taxa linked by similar fermentative and methanogenic metabolic processes. These results demonstrate recurrent associations between specific taxa in the gut microbiota and ethnicity, providing hypotheses for examining specific members of the gut microbiota as mediators of health disparities.

Introduction:

The human gut microbiota at fine resolution varies extensively between individuals (1-3), and this variability frequently associates with diet(4-7), age(6, 8, 9), sex(6, 9, 10), body mass index (BMI) (1, 6), and diseases presenting as health disparities (11-14). The overlapping risk factors and burden of many chronic diseases disproportionally affect ethnic minorities in the United States, yet the underlying biological mechanisms mediating these substantial disparities largely remain unexplained. Recent evidence is consistent with the hypothesis that ethnicity associates with microbial abundance, specifically in the oral cavity, gut, and vagina (15-17). Ethnicity can capture many facets of biological variation including social, economic and cultural variation as well as aspects of human genetic variation and biogeographical ancestry (18, 19). Despite the importance of understanding the interconnections between ethnicity, microbiota, and health disparities, there are no replicated generalizations about the influence of ethnicity on variation in the gut microbiota and specific microbial taxa in diverse American populations, even for healthy individuals (6).

Here, we comprehensively examine connections between self-declared ethnicity and gut microbiota variation in more than a thousand individuals sampled by the American Gut Project (AGP, N=1375) (20) and the Human Microbiome Project (HMP, N=298) (6). Human genetic diversity in the HMP has been shown to associate with differences in microbiota composition, and it has been demonstrated that genetic population structure within the HMP partially delineates self-declared ethnicity (21). Ethnicity was not found to have a significant association with microbiota composition in a middle-eastern population, however microbiota influencing factors such as lifestyle and environment across participants was

67 homogenous compared to the ethnic, sociocultural, economic, and dietary diversity found
68 within the United States (22).
69
70 **Results:**
71 ***Ethnicity subtly demarcates microbiota***
72 We first evaluate gut microbiota distinguishability between AGP ethnicities (**Fig 1A**,
73 family taxonomic level, Asians-Pacific Islanders (N=88), Caucasians (N=1237), Hispanics
74 (N=37), and African Americans (N=13)), sexes (female (N=657), male (N=718)), age groups
75 (years grouped by decade), and categorical BMI (underweight (N=70), normal (N=873),
76 overweight (N=318), and obese (N=114)) (Demographic details in **S1 Table**). 97%
77 Operational Taxonomic Units (OTUs) generated for each dataset are utilized throughout to
78 maintain consistency with other published literature, however microbial taxonomy of the
79 HMP is reassigned using the Greengenes reference database (23). While interindividual
80 microbiota heterogeneity dominates, Analyses of Similarity (ANOSIM) reveal subtle but
81 significant degrees of total microbiota distinguishability for ethnicity, BMI, and sex, but not
82 for age (**Fig 1B**, Ethnicity; **Fig 1C**, BMI; **Fig 1D**, Sex; **Fig 1E**, Age) (24). Recognizing that subtle
83 microbiota distinguishability between ethnicities may be spurious, we independently
84 replicate the ANOSIM results from HMP African Americans (N=10), Asians (N=34),
85 Caucasians (N=211) and Hispanics (N=43) (**S2A Table**, R=0.065, p=0.044), and observe no
86 significant distinguishability for BMI, sex, and age. Higher rarefaction depths increase
87 microbiota distinguishability in the AGP across various beta diversity metrics and
88 categorical factors (**S2B Table**), and significance increases when individuals from
89 overrepresented ethnicities are subsampled from the average beta diversity distance matrix

(**S2C Table**). Supporting the ANOSIM results, Permutational Multivariate Analysis of Variance (PERMANOVA) models with four different beta diversity metrics showed that while all factors had subtle but significant associations with microbiota variation when combined in a single model, effect sizes were highest for ethnicity in 7 out of 8 comparisons across beta diversity metrics and rarefaction depths in the AGP and HMP (**S2D Table**). We additionally test microbiota distinguishability by measuring the correlation between beta diversity and ethnicity, BMI, sex, and age with an adapted BioEnv test (**S2E Table**) (25). Similar degrees of microbiota structuring occur when all factors are incorporated (Spearman Rho=0.055, p-values: Ethnicity=0.057, BMI<0.001, Sex<0.001, Age=0.564). Firmicutes and Bacteroidetes dominated the relative phylum abundance, with each representing between 35% and 54% of the total microbiota across ethnicities (**S1 Fig**).

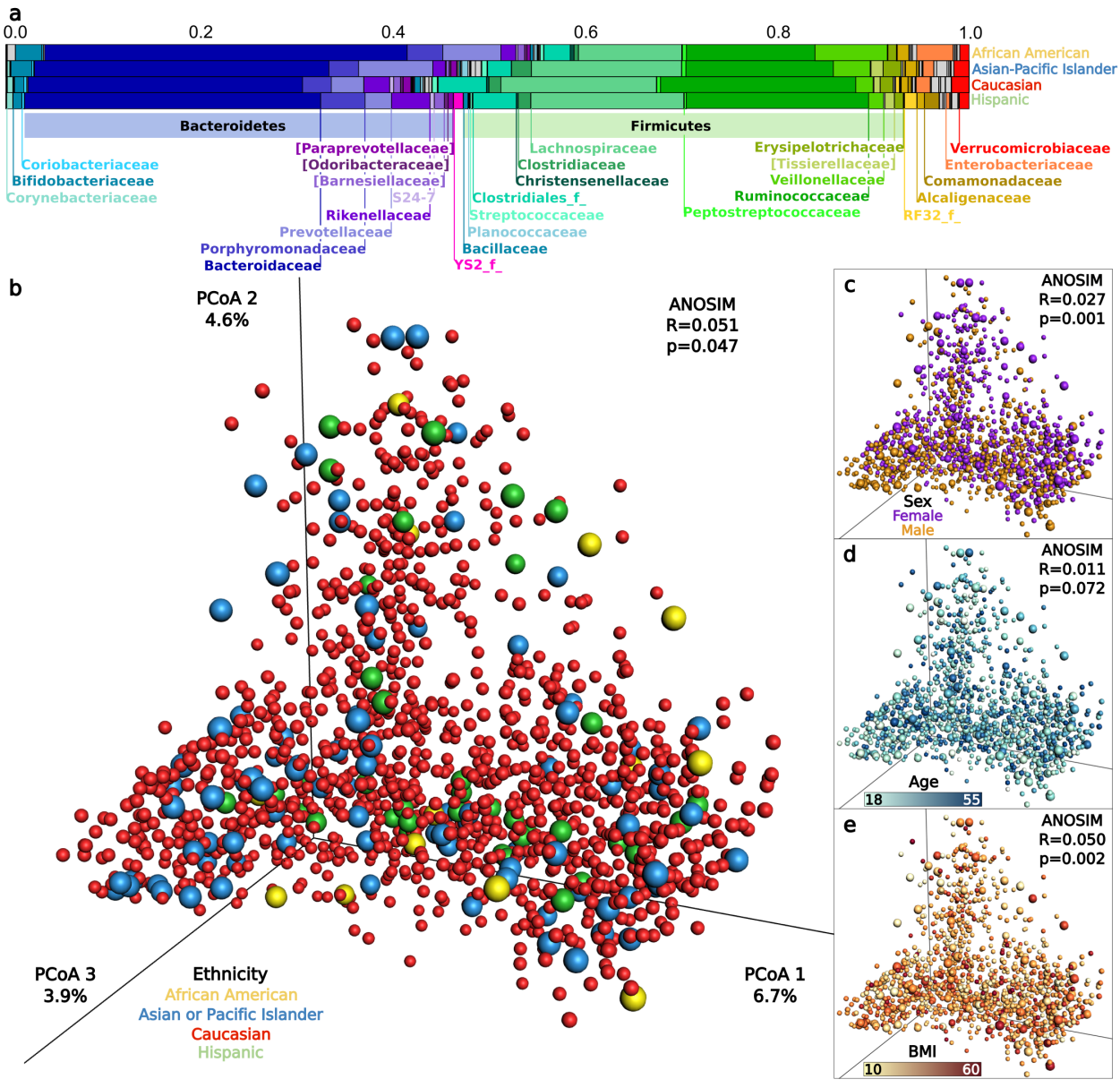

Fig 1. Gut microbiota composition and distinguishability by ethnicity, sex, age and BMI. (A) The average relative abundance of dominant microbial families for each ethnicity. (B-E) Principle coordinates analysis plots of microbiota Bray-Curtis beta diversity and ANOSIM distinguishability for: (B) Ethnicity, (C) Sex, (D) Age, (E) BMI. In B-E, each point represents the microbiota of a single sample, and colors reflect metadata of that individual. Caucasian points are reduced in size to allow clearer visualization.

We next test for ethnicity signatures in the gut microbiota by analyzing alpha and beta diversity, abundance and ubiquity distributions, distinguishability, and classification accuracy (26). Shannon's Alpha Diversity Index (27), which weights both microbial community richness (Observed OTUs) and evenness (Equitability), significantly varies across ethnicities in the AGP dataset (Kruskal Wallis, p=2.8e-8) with the following ranks: Hispanics > Caucasians > Asian-Pacific Islanders > African Americans (**Fig 2A**). Some of these results replicate in the HMP dataset, where we find a significantly lower Shannon diversity for Asian-Pacific Islanders relative to Caucasians, and a trend of lower Shannon diversity for Asian-Pacific Islanders relative to Hispanics. Five alpha diversity metrics, two rarefaction depths, and separate analyses of Observed OTUs and Equitability generally confirm the results (**S3A Table**).

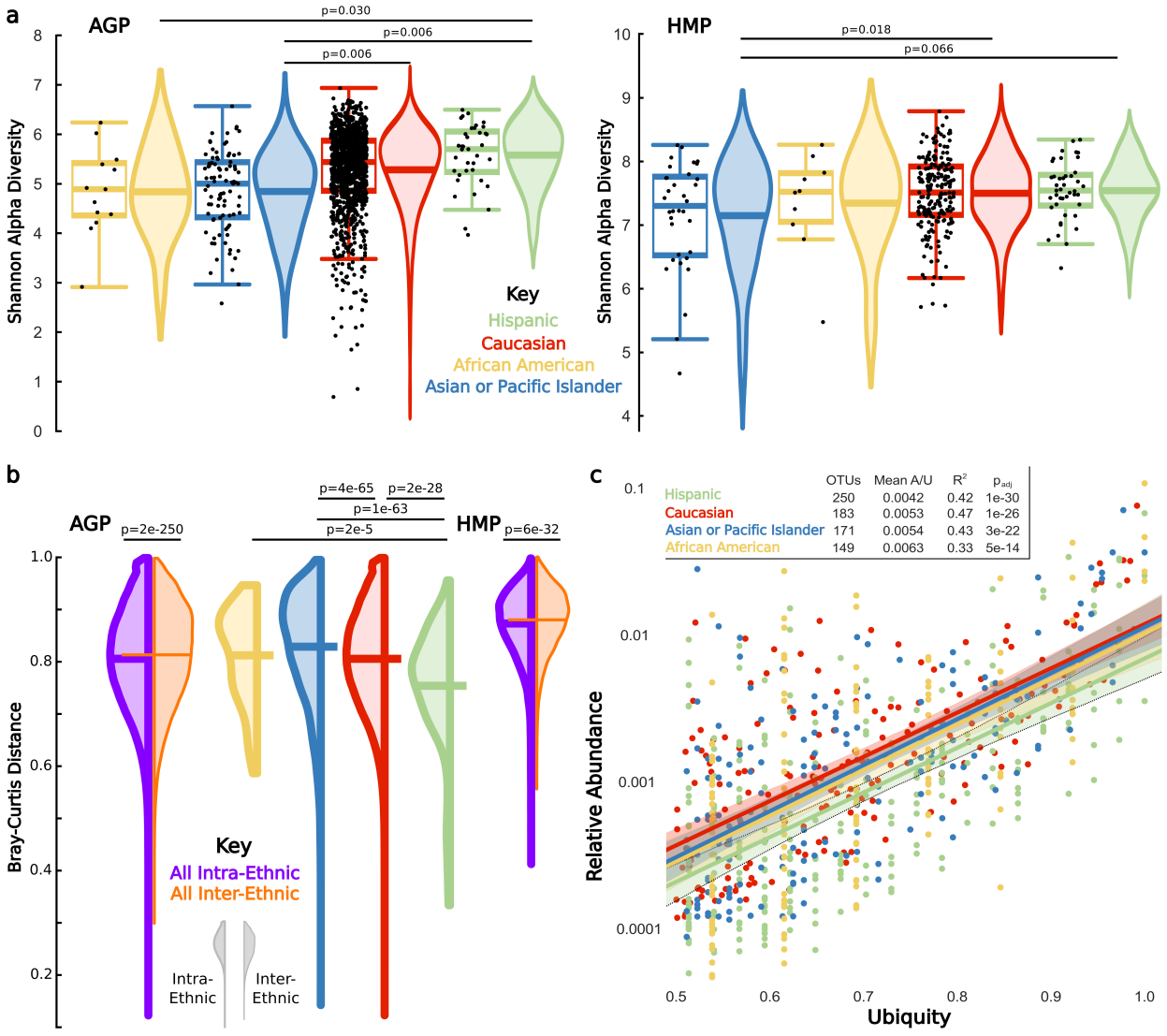

Fig 2. Ethnicity associates with diversity and composition of the gut microbiota. (A) Center lines of each boxplot depict the median by which ethnicities were ranked from low (left) to high (right); the lower and upper end of each box represent the 25th and 75th quartiles respectively; whiskers denote the 1.5 interquartile range, and black dots represent individual samples. Lines in the middle of violin plots depict the mean, and p-values are Bonferroni corrected within each dataset. (B) Left extending violin plots represent intra-ethnic distances for each ethnicity, and right extending violin plots depict all inter-ethnic distances. Center lines depict the mean beta diversity. Significance bars above violin plots

depict Bonferroni corrected pairwise Mann-Whitney-U comparisons of the intra-intra- and intra-inter-ethnic distances. (C) Within each ethnicity, OTUs shared by at least 50% of samples. Colored lines represent a robust ordinary least squares regression within OTUs of each ethnicity, shaded regions represent the 95% confidence interval, R^2 denotes the regression correlation, the OTUs column indicates the number of OTUs with >50% ubiquity for that ethnicity, Mean A/U is the average abundance/ubiquity ratio, and the p_{adj} is the regression significance adjusted and Bonferroni corrected for the number of ethnicities.

If ethnicity impacts microbiota composition, pairwise beta diversity distances (ranging from 0/completely dissimilar to 1/identical) will be greater between ethnicities than within ethnicities. While average gut microbiota beta diversities across all individuals are high (**Fig 2B**, Bray-Curtis=0.808), beta diversities between individuals of the same ethnicity (intra-ethnic, Bray-Curtis=0.806) are subtly, but significantly, lower than those between ethnicities in both the AGP (inter-ethnic, Bray-Curtis=0.814) and HMP datasets (intra-ethnic, Bray-Curtis=0.870 versus inter-ethnic, Bray-Curtis=0.877). We confirm AGP results by subsampling individuals from overrepresented ethnicities across beta metrics and rarefaction depths (**S4A-4B Tables**). Finally, we repeat analyses across beta metrics and rarefaction depths using only the average distance of each individual to all individuals from the ethnicity to which they are compared (**S4C-4D Tables**).

Next, we explore inter-ethnic variation in the number of OTUs shared in at least 50% of individuals within an ethnicity. Out of 5,591 OTUs in the total AGP dataset, 101 (1.8%) meet this ubiquity cutoff in all ethnicities, and 293 (5.2%) unique OTUs meet the cutoff within at least one ethnicity. Hispanics share the most ubiquitous OTUs and have the lowest

152 average abundance/ubiquity (A/U) ratio (**Fig 2C**), indicating higher stability of lower
153 abundance shared OTUs (28). This result potentially explains their significantly lower intra-
154 ethnic beta diversity distance and thus higher microbial community overlap relative to the
155 other ethnicities (**Fig 2B**). Comparisons in the AGP between the higher sampled Hispanic,
156 Caucasian, and Asian-Pacific Islander ethnicities also reveal a trend wherein higher intra-
157 ethnic community overlap (**Fig 2B**) parallels higher numbers of ubiquitous OTUs (**Fig 2C**),
158 higher Shannon Alpha diversity (**Fig 2A**), and higher stability of ubiquitous OTUs as
159 measured by the abundance/ubiquity (A/U) ratio (**Fig 2C**).

160 We next assess whether a single ethnicity disproportionately impacts total gut
161 microbiota distinguishability in the AGP by comparing ANOSIM results from the consensus
162 beta diversity distance matrix when each ethnicity is sequentially removed from the analysis
163 (**Fig 3A** and **S2E Table**). Distinguishability remains unchanged when the few African
164 Americans are removed, but is lost upon removal of Asian-Pacific Islanders or Caucasians
165 (**Fig 3A**). Notably, removal of Hispanics increases distinguishability among the remaining
166 ethnicities, which may be due to higher degree of beta diversity overlap observed between
167 Hispanics and other ethnicities (**S4B Table**). Results conform across rarefaction depths and
168 beta diversity metrics (**S2F Table**), and pairwise combinations show strong
169 distinguishability between African Americans and Hispanics (ANOSIM, $R=0.234$, $p=0.005$),
170 and Asian-Pacific Islanders and Caucasians (ANOSIM, $R=0.157$, $p<0.001$).

171 Finally, to complement evaluation with ecological alpha and beta diversity we
172 implement a random forest supervised learning algorithm to classify gut microbiota from
173 genus level community profiles into their respective ethnicity. We build four one-versus-all
174 binary classifiers to classify samples from each ethnicity compared to the rest, and use two

different sampling approaches to train the models, Synthetic Minority Over-sampling Technique (SMOTE) (29) and down-sampling, for overcoming uneven representation of ethnicities in both the datasets (see Methods). Given that the area under the receiver operating characteristic (ROC) curve (or AUC) of a random guessing classifier is 0.5, the models classify each ethnicity fairly well (**Fig 3B**) with average AUCs across sampling techniques and datasets of 0.78 for Asian-Pacific Islanders, 0.76 for African Americans, 0.69 for Hispanics, and 0.70 for Caucasians.

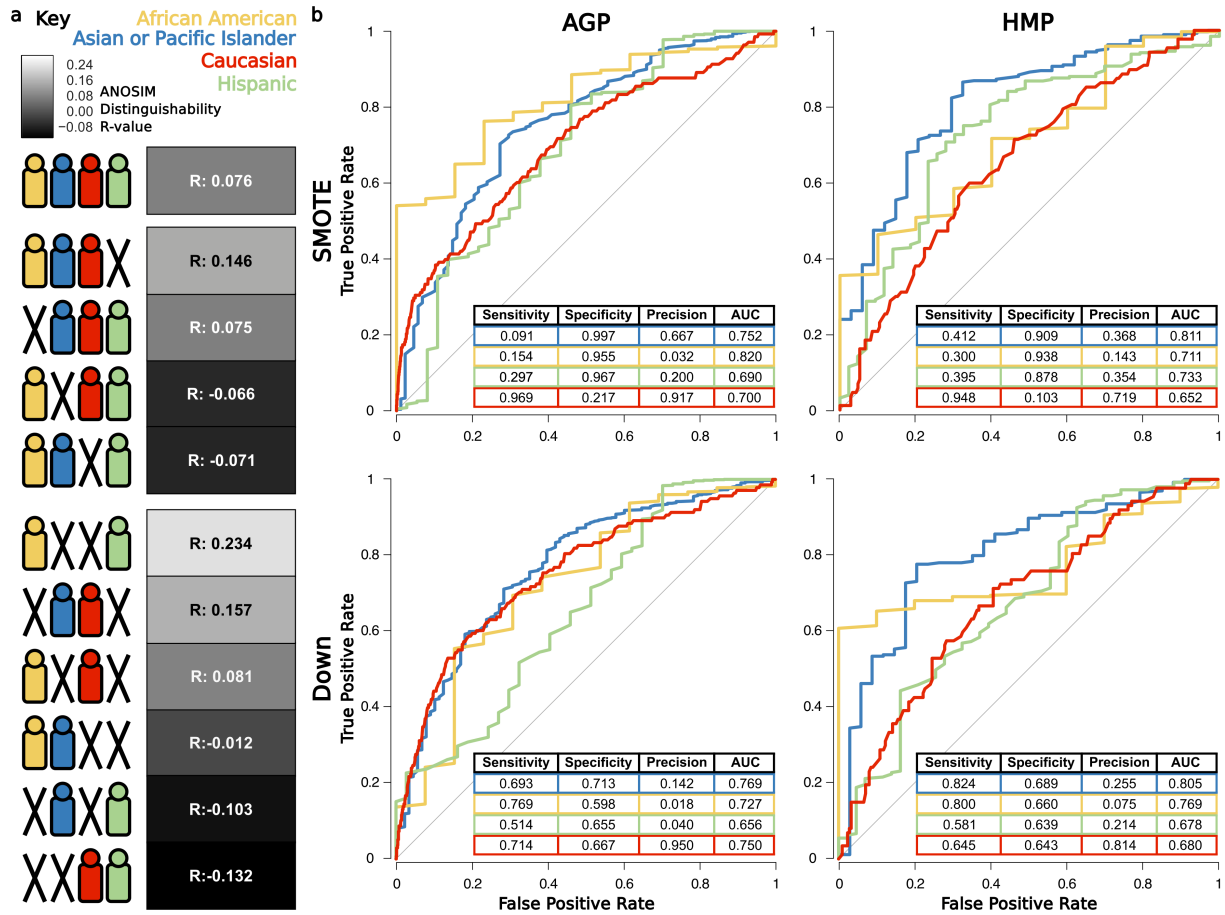

Fig 3. Microbiota distinguishability and classification ability across ethnicities. (A) ANOSIM distinguishability between all combinations of ethnicities. Symbols depict specific ethnicities included in the ANOSIM tests, and boxes denote the R-value as a heatmap, where

186 white indicates increasing and black indicates decreasing distinguishability relative to the R-
187 value with all ethnicities. (B) Average ROC curves (for 10-fold cross-validation) and
188 prediction performance metrics for one-versus-all random forest classifiers for each
189 ethnicity, using SMOTE (29) and down subsampling approaches for training.
190
191 ***Recurrent taxa associations with ethnicity***
192 Subtle to moderate ethnicity-associated variation in microbial communities may in
193 part be strongly driven by differential abundance of certain microbial lineages. We find that
194 16.2% (130/802) of the AGP taxa and 20.6% (45/218) of HMP taxa across all classification
195 levels (i.e. phylum to genus, **S5 Table**) significantly vary in abundance across ethnicities
196 (Kruskal-Wallis, $p_{FDR}<0.05$). Between datasets, 19.2% (25/130) of the AGP and 55.6%
197 (25/45) of the HMP varying lineages replicate in the other dataset, representing a
198 significantly greater degree of overlap than would be expected by chance (AGP replicated,
199 Fisher's exact one-tailed test, expected 5% overlap (7 overlapping vs. 123 not overlapping)
200 and observed (25 overlapping vs. 105 not overlapping), p=5.26e-4; HMP replicated, Fisher's
201 exact test, expected 5% overlap (2 overlapping vs. 43 not overlapping) and observed (25
202 overlapping vs. 20 not overlapping), p=4.72e-8; ethnic permutation analysis of overlap,
203 p<0.001 each taxonomic level and all taxonomic levels combined). The highest replication of
204 taxonomic lineages varying by abundance occurs with 22.0% (9/41) of families across
205 datasets, followed by genus with 13.4% (9/67).
206 Among 18 reproducible lineages, we categorize 12 as unique (**Fig 4**) and exclude 6
207 where nearly identical abundance profiles between family/genus taxonomy overlap.
208 Comparing relative abundance differences between pairs of ethnicities for these 12 taxa in

AGP and HMP reveals 20 out of 30 significant ($p<0.05$, Mann-Whitney-U) differences replicated. Intriguingly, all reproducible pairwise differences are a result of decreases in Asian-Pacific Islanders (**Fig 4**).

We also test taxon abundance and presence/absence associations with ethnicity separately in the AGP using linear and logistic regression models respectively, and we repeat the analysis while incorporating categorical sex and continuous age and BMI as covariates (**S6 Table**). Clustering microbial families based on their abundance correlation reveals two co-occurrence clusters: (i) a distinct cluster of six Firmicutes and Tenericutes families in the HMP and (ii) an overlapping but more diverse cluster of 20 families in the AGP (**S2 Fig**). Nine of the 12 taxa found to recurrently vary in abundance across ethnicities are represented in these clusters (**Fig 4**), with four appearing within both clusters, and the other five appearing either within or closely correlated with members of both clusters (**S2 Fig**). Further, 90% (18/20) of families in the AGP cluster and 66% (4/6) of taxa in the HMP cluster significantly vary in abundance across ethnicities. Taken together, these results establish general overlap of the most significantly ethnically-associated taxa between the three methods, reproducibility of microbial abundances that vary between ethnicities across datasets, and patterns of co-occurrence among these taxa which could suggest they are functionally linked.

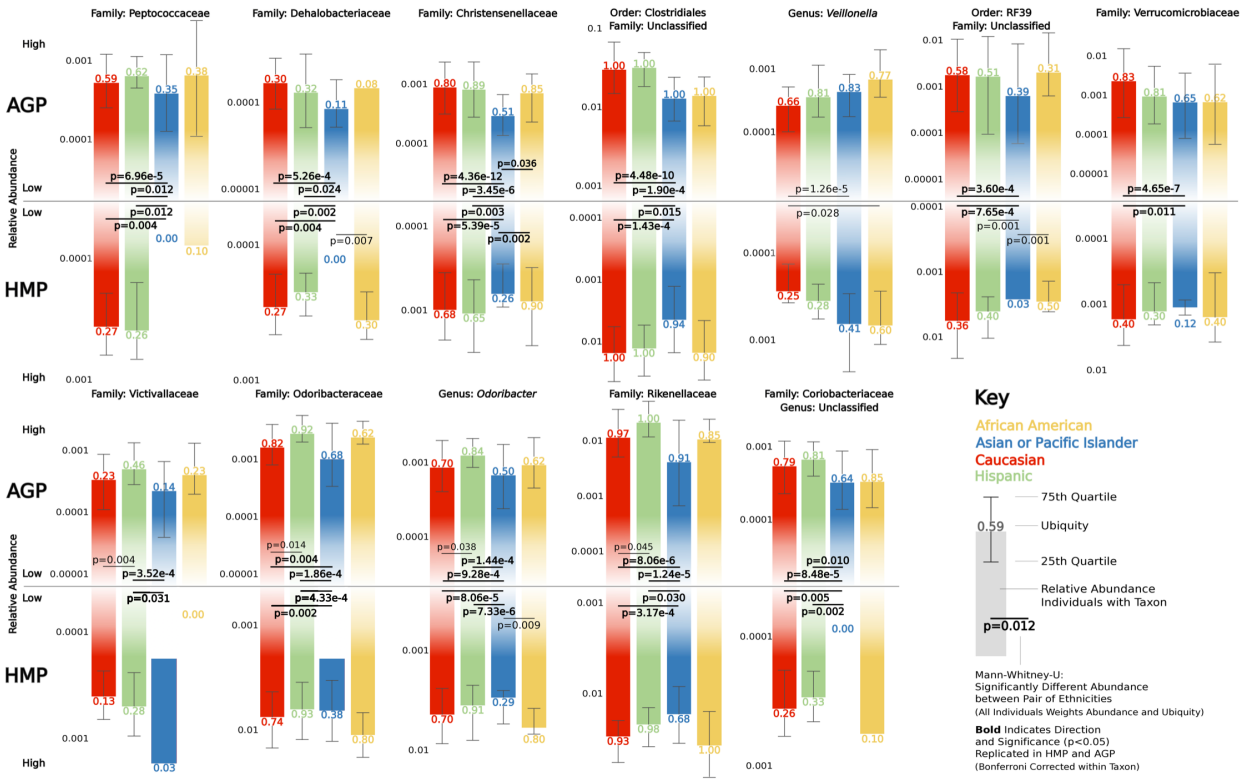

Fig 4. Ethnicity-associated taxa match between the HMP and AGP. Barplots depict the log10 transformed relative abundance for individuals possessing the respective taxon within each ethnicity, ubiquity appears above (AGP) or below (HMP) bars, and the 25th and 75th percentiles are shown with extending whiskers. Mann-Whitney-U tests evaluate differences in abundance and ubiquity for all individuals between pairs of ethnicities; for example, the direction of change in Victivallaceae is driven by ubiquity while abundance is higher for those possessing the taxon. Significance values are Bonferroni corrected for the six tests within each taxon and dataset, and bold p-values indicate that significance ($p<0.05$) and direction of change replicate in the AGP and HMP.

Most heritable taxon varies by ethnicity

Identified as the most heritable human gut taxon (30, 31), the family Christensenellaceae exhibits the second strongest significant differences in abundance across ethnicities in both AGP and HMP datasets (**S5 Table**, Family: AGP, Kruskal-Wallis, p_{FDR}=1.55e-9; HMP, Kruskal-Wallis, p_{FDR}=0.0019). Additionally, Christensenellaceae is variable by sex and BMI (AGP: Sex, Kruskal-Wallis, p_{FDR}=1.22e-12; BMI, Kruskal-Wallis, p_{FDR}=0.0020), and represents some of the strongest pairwise correlations with other taxa in both co-occurrence clusters (**S2 Fig**). There is at least an eight-fold and two-fold reduction in average Christensenellaceae abundance in Asian-Pacific Islanders relative to the other ethnicities in the AGP and HMP respectively (**S5 Table**), and significance of all pairwise comparisons in both datasets show reduced abundance in Asian-Pacific Islanders (**Fig 4**). Abundance in individuals possessing Christensenellaceae and presence/absence across all individuals significantly associate with ethnicity (**S6 Table**, Abundance, Linear Regression, $p_{Bonferroni}$=0.006; Presence/Absence, Logistic Regression, $p_{Bonferroni}$=8.802e-6), but there was only a slight correlation between the taxon's relative abundance and BMI (**S3 Fig**). Confirming previous associations with lower BMI(32), we observe that AGP individuals with Christensenellaceae also have a significantly lower BMI (Mean BMI, 23.7±4.3) than individuals without it (Mean BMI, 25.0±5.9; Mann-Whitney-U, $p<0.001$). This pattern is separately reflected in African Americans, Asian-Pacific Islanders, and Caucasians but not Hispanics (**Fig 5**), suggesting that each ethnicity may have different equilibria between the taxon's abundance and body weight.

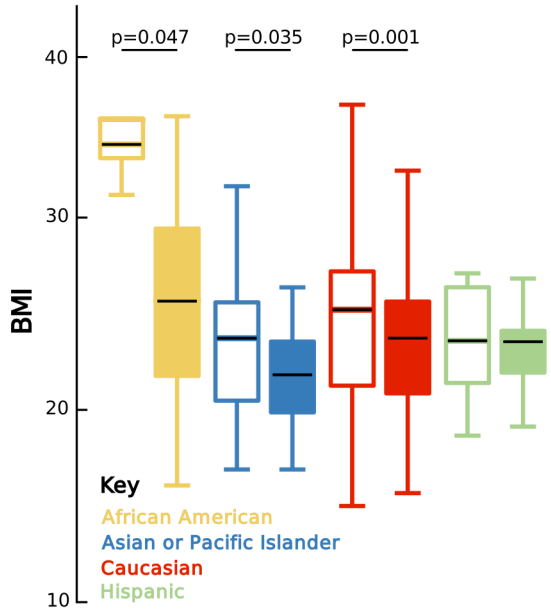

Fig 5. Christensenellaceae variably associates with BMI across ethnicities. Boxplots of BMI for individuals without (unfilled boxplots) and with (filled boxplots) Christensenellaceae. Significance was determined using one-tailed Mann-Whitney-U tests for lower continuous BMI values. Black lines indicate the mean relative abundance; the lower and upper end of each box represent the 25th and 75th quartiles respectively; and whiskers denote the 1.5 interquartile range.

Genetic- and ethnicity-associated taxa overlap

Many factors associate with human ethnicity, including a small subset of population specific genetic variants (estimated ~0.5% genome wide) that vary by biogeographical ancestry (33, 34), and self-declared ethnicity in the HMP is delineated by population genetic structure (21). Here we investigate whether ethnicity-associated taxa overlap with (i) taxa that have a significant population genetic heritability in humans (30, 31, 35, 36) and (ii) taxa linked with human genetic variants in two large Genome-Wide Association Studies (GWAS)-

273 microbiota analyses (31, 36). All except one recurrent ethnicity-associated taxa are heritable
274 in at least one study, with seven replicating in three or more studies (**Table 1**). Likewise,
275 abundance variation in seven recurrent ethnicity-associated taxa demonstrate significant
276 GWAS associations with at least one variant in the human genome, therefore we assess
277 whether any genetic variants associated with differences in microbial abundance show
278 significant rates of differentiation (F_{ST}) between 1,000 genomes superpopulations (34). Out
279 of 49 variants associated with ethnically varying taxa, 21 have higher F_{ST} values between at
280 least one pair of populations than that of 95% of other variants on the same chromosome
281 and across the genome, and the F_{ST} values of five variants associated with Clostridiaceae
282 abundance rank above the top 99% (**S7 Table**). Since taxa that vary across ethnicities exhibit
283 lower abundance in Asian-Pacific Islanders, it is notable that the F_{ST} values of 18 and 11
284 variant comparisons for East Asian and South Asian populations, respectively, are above that
285 of the 95% rate of differentiation threshold from African, American, or European
286 populations. Critically, the microbiota and 1,000 genomes datasets are not drawn from the
287 same individuals, and disentangling the role of genetic from social and environmental factors
288 will still require more controlled studies.
289

Recurrent Ethnicity-Associated Taxa	Heritability	Genetic Associations
Family: Peptococcaceae	0.1213[A], 0.2154[C], 0.26[E]	rs143179968[E]
Family: Dehalobacteriaceae	0.6878[B], 0.3087[C]	
Family: Christensenellaceae	0.3819 [A], 0.6170[B], 0.4230[C],	
Order: Clostridiales, Family: Unclassified	0.2914[A], 0.4020[B], 0.1330[C]	*40 Genetic Variants[C]
Genus: *Veillonella*	0.1370[A], 0.2168[D]	rs347941[C]
Order: RF39, Family: Unclassified	0.2341[A], 0.6618[B], 0.3074[C]	rs4883972[C]
Family: Verrucomicrobiaceae	0.1257[A], 0.5973[B], 0.1394[C]	
Family: Victivallaceae		
Family Odoribacteraceae	0.1389[A], 0.1917[D], 0.34[E]	chr7:96414393[E], rs115795847[E]
Genus: *Odoribacter*	0.1916[D]	
Family: Rikenellaceae	0.1299[D], 0.29[E]	rs17098734[C], rs3909540[C], rs147600757[E],
Family: Coriobacteraceae, Genus:	0.1364[A], 0.2822[B], 0.1609[C]	rs9357092[E]

290

Table 1. Recurrent ethnicity-associated taxa overlap heritable and genetically-associated taxa. The table shows population genetic heritability estimates and associated genetic variants for the 12 recurrent ethnically varying taxa. The minimum heritability cutoff was chosen as >0.1, and only exactly overlapping taxonomies were considered. Studies examined: [A]UKTwins (2014, A in ACE model) (30), [B]Yatsunenko (2014, A in ACE model) (30), [C]UKTwins (2016, A in ACE model) (31), [D]Lim (2016, H2r in SOLAR (37)) (35), [E]Turpin (2016, H2r in SOLAR (37)). *indicates excessive variants were excluded from table.

Discussion:

Many common diseases associate with microbiota composition and ethnicity, raising the central hypothesis that microbiota variation between ethnicities can occasionally serve as a mediator of health disparities. American's self-declared ethnicity can capture socioeconomic, cultural, geographic, dietary and genetic diversity, and a similarly complex array of interindividual and environmental factors influence total microbiota composition, resulting in challenges when trying to consistently recover variation in total gut microbiota between ethnicities. These challenges inform the importance of reproducibility, both through confirmation across analytical methods and replication across study populations. In order to more fully evaluate this hypothesis, baseline generalizations are drawn here about the impact of ethnicity on gut microbiota variation in healthy individuals, and is concordant with recent literature in single populations suggesting that ethnicity plays a subtle but reproducible role in microbiota assembly (15-17, 21, 22).

Whether shaped through socioeconomic, dietary, healthcare, genetic, or other ethnicity-related factors, the replicated, varying taxa represent sources for novel hypotheses

addressing health disparities. For instance, the family Odoribacteraceae and genus *Odoribacter* are primary butyrate producers in the gut, and have been negatively linked to severe forms of Crohn's disease and Ulcerative Colitis in association with reduced butyrate metabolism (38-40). Asian-Pacific Islanders possess significantly less Odoribacteraceae and *Odoribacter* than Hispanics and Caucasians in both datasets, and severity of Ulcerative Colitis upon hospital admission has been shown to be significantly higher in Asian Americans (41). Considering broader physiological roles, several ethnicity-associated taxa are primary gut anaerobic fermenters and methanogens (42, 43), and associate with lower BMI and blood triglyceride levels (32, 44). Indeed, Christensenellaceae, Odoribacteraceae, *Odoribacter*, and the class Mollicutes containing RF39 negatively associate with metabolic syndrome and demonstrate significant population heritability in twins (35). Implications for health outcomes warrant further investigation, but could be reflected by positive correlations of Odoribacteraceae, *Odoribacter*, Coriobacteriaceae, Christensenellaceae, and the dominant Verrucomicrobiaceae lineage *Akkermansia* with old age (45, 46). Moreover, these findings raise the importance of controlling for ethnicity in studies linking microbiota variation to disease because associations between specific microbes and a disease could be confounded by ethnicity of the study subjects.

Based on correlations in individual taxon's abundance, a similar pattern of co-occurrence previously identified as the Christensenellaceae 'consortium' includes 11 of the 12 recurrent ethnically varying taxa (30), and members of this consortium associate with genetic variation in the human formate oxidation gene *ALDH1L1* which is a genetic risk factor for stroke (31, 47, 48). Formate metabolism is a key step in the pathway reducing carbon dioxide to methane (49, 50), and increased methane associates with increased Rikenellaceae,

337 Christensenellaceae, Odoribacteraceae and *Odoribacter* (51). Products of methanogenic
338 fermentation pathways include short chain fatty acids such as butyrate, which through
339 reduction of pro-inflammatory cytokines has been linked to cancer cell apoptosis and
340 reduced risk of colorectal cancer (52, 53). Asian Americans are the only ethnic group where
341 cancer surpasses heart disease as the leading cause of death, and over 70% of Asian
342 Americans were born overseas, which can affect assimilation into western lifestyles, leading
343 to reduced access to healthcare and screening, and proper medical education (52, 54-56).
344 Indeed, as countries in Asia shift toward a more western lifestyle, the incidence of cancers,
345 particularly gastrointestinal and colorectal cancers, are increasing rapidly, possibly
346 indicating incompatibilities between traditionally harbored microbiota and western
347 lifestyles (57-60). Asian Americans have higher rates of type 2 diabetes and pathogenic
348 infections than Caucasians (61), and two metagenomic functions enriched in control versus
349 type 2 diabetes cases appear to be largely conferred by cluster-associated butyrate-
350 producing and motility-inducing Verrucomicrobiaceae and Clostridia lineages reduced in
351 abundance among AGP and HMP Asian-Pacific Islanders (11). Both induction of cell motility
352 and butyrate promotion of mucin integrity can protect against pathogenic colonization and
353 associate with microbial community changes (11, 53, 62). Levels of cell motility and butyrate
354 are key factors suspected to underlie a range of health disparities including inflammatory
355 bowel disease, arthritis, and type 2 diabetes (11, 63-65). Patterns of ethnically varying taxa
356 across ethnicities could result from many factors including varying diets, environmental
357 exposures, sociocultural influences, human genetic variation and others. However,
358 regardless of the mechanisms dictating assembly, these results suggest there is a

359 reproducible, co-occurring group of taxa linked by similar metabolic processes known to
360 promote homeostasis.

361 The utility of this work is establishing a framework for studying ethnicity-associated
362 taxa and hypotheses of how changes in abundance or presence of these taxa may or may not
363 shape health disparities, many of which also have genetic components. Differing in allele
364 frequency across three population comparisons and associated with the abundance of
365 Clostridiales, the genetic variant rs7587067 has a significantly higher frequency in African
366 (Minor Allele Frequency (MAF)=0.802) versus East Asian (MAF=0.190, F_{ST}=0.54,
367 Chromosome=98.7%, Genome-Wide=98.9%), admixed American (MAF=0.278, F_{ST}=0.44,
368 Chromosome=99.0%, Genome-Wide=99.1%), and European populations (MAF=0.267,
369 F_{ST}=0.45, Chromosome=98.7.3%, Genome-Wide=98.7%). This intronic variant for the gene
370 *HECW2* is a known eQTL (GTeX, eQTL Effect Size=-0.18, p=7.4e-5) (66, 67), and *HECW2*
371 encodes a ubiquitin ligase linked to enteric gastrointestinal nervous system function through
372 maintenance of endothelial lining of blood vessels (68, 69). Knockout of *HECW2* in mice
373 reduced enteric neuron networks and gut motility, and patients with Hirschsprung's disease
374 have diminished localization of *HECW2* to regions affected by loss of neurons and colon
375 blockage when compared to other regions of their own colon and healthy individuals (70).
376 Hirschsprung's disease presenting as full colon blockage is rare and has not undergone
377 targeted examination as a health disparity, however a possible hypothesis is that lower
378 penetrance of the disease in individuals with the risk allele at rs7587067 could lead to
379 subtler effects on gut motility resulting in Clostridiales abundance variation.

380 Another example is that the abundance of Rikenellaceae in the gut is strongly and
381 reproducibly associated with variant rs62171178, which was identified as an eQTL for gene

382 *PHOSPHO2* within human gut tissue (36, 67). The primary substrate of the protein encoded
383 by *PHOSPHO2* is vitamin B6 (71), which shows increased deficiencies in germ free compared
384 to conventionally reared rats (72). Interestingly, microbial vitamin B6 biosynthesis and
385 salvage was the best predictor of chronic fatigue and irritable bowel syndromes (73, 74).
386 Despite the intrigue of connecting the human genome, microbiota and disease phenotypes,
387 evaluating these hypotheses will require more holistic approaches such as incorporating
388 metagenomics and metabolomics to identify whether enzymes or metabolic functions
389 reproducibly vary across ethnicities, as well as direct functional studies in model systems to
390 understand if correlation is truly driven by causation.

391 Further limitations should also be considered, including recruitment biases for the
392 AGP versus HMP, variation in sample processing and OTU clustering, and uneven sampling
393 which could only be addressed with down sampling of over-represented ethnicities. Still,
394 despite these confounders care was taken to demonstrate the reproducibility of results
395 across statistical methods, ecological metrics, rarefaction depths, and study populations.
396 Summarily, this work suggests that abundance variation of specific taxa, rather than whole
397 communities, may represent the most reliable ethnic signatures in the gut microbiota. A
398 reproducible co-occurring subset of these taxa link to a variety of overlapping metabolic
399 processes and health disparities, and contain the most heritable bacterial family,
400 Christensenellaceae. Moreover, a majority of the microbial taxa associated with ethnicity are
401 also heritable and genetically-associated lineages, suggesting there is a possible connection
402 between ethnicity and genetic patterns of biogeographical ancestry that may play a role in
403 shaping these taxa. Our results emphasize the importance of sampling ethnically diverse
404 populations of healthy individuals in order to discover and replicate ethnicity signatures in

405 the human gut microbiota, and they highlight a need to account for ethnic variation as a
406 potential confounding factor in studies linking microbiota variation to disease. Further
407 reinforcement of these results may lead to generalizations about microbiota assembly and
408 even consideration of specific taxa as potential mediators or treatments of health disparities.

Materials and Methods:

Data Acquisition

AGP data was obtained from the project FTP repository located at *ftp://ftp.microbio.me/AmericanGut/*. AGP data generation and processing prior to analysis can be found at: *https://github.com/biocore/American-Gut/tree/master/ipynb/primary-processing*. All analyses utilized the rounds-1-25 dataset which was released on March 4, 2016. Throughout all analyses, QIIME v1.9.0 was used in an Anaconda environment [*https://continuum.io*] for all script calls, custom scripts and notebooks were run in the QIIME 2 Anaconda environment with python version 3.5.2, and plots were post-processed using Inkscape [*https://inkscape.org/en/*] (75). Ethnicity used in this study was self-declared by AGP study participants as one of four groups: African American, Asian or Pacific Islander (Asian-Pacific Islander), Caucasian, or Hispanic. Sex was self-declared as either male, female, or other. Age was self-declared as a continuous integer of years old, and age categories defined by the AGP by decade (i.e. 20's, 30's…) were used in this study. BMI was self-declared as an integer, and BMI categories defined by AGP of underweight, healthy, overweight, and obese were utilized. Microbiota communities were characterized using 16S rDNA sequencing of variable region four and OTU clustering at 97% similarity, following an identical processing pipeline for all samples developed and optimized for the Earth Microbiome Project (76). HMP 16S rDNA data processed using QIIME for variable regions 3-5 was obtained from *http://hmpdacc.org/HMQCP/*. Demographic info for individual HMP participants was obtained through dbGaP restricted access to study phs000228.v2.p1, with dbGaP approval granted to SRB and non-human subjects determination IRB161231 granted by Vanderbilt University. Ethnicity and sex were assigned to subjects based on self-declared

values, with individuals selecting multiple ethnicities being removed unless they primarily responded as Hispanic, while categorical age and BMI were established from continuous values using the same criteria for assignment as in AGP. The HMP Amerindian population was removed due to severe under-representation. This filtered HMP table was used for community level analyses (ANOSIM, Alpha Diversity, beta intra-inter), however to allow comparison with the AGP dataset, community subset analyses (co-occurrence, abundance correlation, etc…) were performed with taxonomic assignments in QIIME using the UCLUST method with the GreenGenes_13_5 reference.

Quality Control

AGP quality control was performed in Stata v12 (StataCorp, 2011) using available metadata to remove samples (Raw N=9,475): with BMI more than 60 (-988 [8,487]) or less than 10 (-68 [8,419]), missing age (-661 [7,758]), with age greater than 55 years old (-2,777 [4,981]) or less than 18 years old (-582 [4,399]), and blank samples or those not appearing in the mapping file (-482 [3,917]), with unknown ethnicity or declared as other (-131 [3786]), not declared as a fecal origin (-2,002 [1784]), with unknown sex or declared as other (-98 [1686]), or located outside of the United States (-209 [1477]). No HMP individuals were missing key metadata or had other reasons for exclusion (-0[298]). Final community quality control for both AGP and HMP was performed by filtering OTUs with less than 10 sequences and removing samples with less than 1,000 sequences (AGP, -102 [1375]; HMP, -0 [298]). All analyses used 97% OTUs generated by the AGP or HMP, and unless otherwise noted, results represent Bray-Curtis beta diversity and Shannon alpha diversity at a rarefaction depth of 1,000 counts per sample.

455

456 *ANOSIM, PERMANOVA, and BioEnv Distinguishability*

457 The ANOSIM test was performed with 9,999 repetitions on each rarefied table within
458 a respective rarefaction depth and beta diversity metric (**Fig 1 & S2A-B Table**), with R-
459 values and p-values averaged across the rarefactions. Consensus beta diversity matrices
460 were calculated as the average distances across the 100 rarefied matrices for each beta
461 diversity metric and depth. Consensus distance matrices were randomly subsampled ten
462 times for subset number of individuals from each ethnic group with more than that subset
463 number prior to ANOSIM analysis with 9,999 repetitions, and the results were averaged
464 evaluating the effects of more even representations for each ethnicity (**S2C Table**).
465 Consensus distance matrices had each ethnicity and pair of ethnicities removed prior to
466 ANOSIM analysis with 9,999 repetitions, evaluating the distinguishability conferred by
467 inclusion of each ethnicity (**Fig 3A**, **S2F Table**). Significance was not corrected for the
468 number of tests to allow comparisons between results of different analyses, metrics, and
469 depths. PERMANOVA analyses were run using the R language implementation in the Vegan
470 package (77), with data handled in a custom R script using the Phyloseq package (78).
471 Categorical variables were used to evaluate the PERMANOVA equation (Beta-Diversity
472 Distance Matrix ~ Ethnicity + Age + Sex + BMI) using 999 permutations to evaluate
473 significance, and the R and p values were averaged across 10 rarefactions (**S2D Table**). The
474 BioEnv test, or BEST test, was adapted to allow evaluation of the correlation and significance
475 between beta diversity distance matrices and age, sex, BMI, and ethnicity simultaneously
476 (**S2E Table**) (25). At each rarefaction depth and beta diversity metric the consensus distance
477 matrix was evaluated for its correlation with the centered and scaled Euclidian distance

matrix of individuals continuous age and BMI, and categorical ethnicity and sex encoded using patsy (same methodology as original test)[*https://patsy.readthedocs.io/en/latest/#*]. The test was adapted to calculate significance for a variable of interest by comparing how often the degree of correlation with all metadata variables (age, sex, BMI, ethnicity) was higher than the correlation when the variable of interest was randomly shuffled between samples 1,000 times.

Alpha Diversity

Alpha diversity metrics (Shannon, Simpson, Equitability, Chao1, Observed OTUs) were computed for each rarefied table (QIIME: alpha_diversity.py), and results were collated and averaged for each sample across the tables (QIIME: collate_alpha.py). Pairwise nonparametric t-tests using Monte Carlo permutations evaluated alpha diversity differences between the ethnicities with Bonferroni correction for the number of comparisons (**Fig 2A**, **S3 Table**, QIIME: compare_alpha_diversity.py). A Kruskal-Wallis test implemented in python was used to detect significant differences across all ethnicities.

Beta Diversity

Each consensus beta diversity distance matrix had distances organized based on whether they represented individuals of the same ethnic group, or were between individuals of different ethnic groups. All values indicate that all pairwise distances between all individuals were used (**Fig 2B**, **S4A-B Table**), mean values indicate that for each individual their average distance to all individuals in the comparison group was used as a single point to assess pseudo-inflation (**S4C-D Table**). A Kruskal-Wallis test was used to calculate

501 significant differences in intra-ethnic distances across all ethnicities. Pairwise Mann-
502 Whitney-U tests were calculated between each pair of intra-ethnic distance comparisons,
503 along with intra-versus-inter ethnic distance comparisons. Significance was Bonferroni
504 corrected within the number of intra-intra-ethnic and intra-inter-ethnic distance groups
505 compared, with violin plots of intra- and inter-ethnic beta diversity distances generated for
506 each comparison.
507
508 *Random Forest*
509 RF models were implemented using taxa summarized at genus level, which
510 performed better compared to RF models using OTUs as features, both in terms of
511 classification accuracy and computational time. We first rarefied OTU tables at sequence
512 depth of 10,000 (using R v3.3.3 package *vegan's* rrarefy() function) and then summarized
513 rarefied OTUs at genus-level (or lower characterized level if genus was uncharacterized for
514 an OTU). We filtered for rare taxa by removing taxa present in fewer than half of the number
515 of samples in rarest ethnicity (i.e. fewer than 10/2 = 5 samples in HMP and 13/2 = 6 (rounded
516 down) in AGP), retaining 85 distinct taxa in HMP dataset and 322 distinct taxa in AGP dataset
517 at genus level. The resulting taxa were normalized to relative abundance and arcsin-sqrt
518 transformed before being used as features for the RF models. We initially built multi-class
519 RF model, but since the RF model is highly sensitive to the uneven representation of classes,
520 all samples were identified as the majority class, i.e. Caucasian. In order to even out the class
521 imbalance, we considered some sampling approaches, but most existing techniques for
522 improving classification performance on imbalanced datasets are designed for binary class
523 imbalanced datasets, and are not effective on datasets with multiple underrepresented

524 classes. Hence, we adopted the binary classification approach and built four one-versus-all
525 (OVA) binary RF classifiers to classify samples from each ethnicity compared to the rest. 10-
526 fold cross-validation (using R package *caret* (79)) was performed using ROC as the metric
527 for selecting optimal model. The performance metrics and ROC curves were averaged across
528 the 10 folds (**Fig 3B**). Without any sampling during training the classifiers, most samples
529 were identified as the majority class, i.e. the Caucasian, by all four OVA RF classifiers. In order
530 to overcome this imbalance in class representation, we applied two sampling techniques
531 inside cross-validation: i) down-sampling, and ii) Synthetic Minority Over-sampling
532 Technique (or SMOTE) (29). In the down-sampling approach, the majority class is down-
533 sampled by random removal of instances from the majority class. In the SMOTE approach,
534 the majority class is down-sampled and synthetic samples from the minority class are
535 generated based on k-nearest neighbors technique (29). Note, the sampling was performed
536 inside cross-validation on training set, while the test was performed on unbalanced held-out
537 test set in each fold. The ROC curves and performance metrics table in **Fig 3B** show the
538 sensitivity-specificity tradeoff and classification performance for OVA classifier for each
539 ethnicity for both the sampling techniques applied on both the datasets. For both the
540 datasets, down-sampling shows higher sensitivity and lower specificity and precision for
541 minority classes (i.e. African Americans, Asian-Pacific Islanders and Hispanics) compared to
542 SMOTE. However, for the majority class (i.e. Caucasian), down-sampling lowers the
543 sensitivity and increases the specificity and precision compared to SMOTE. The sensitivity-
544 specificity tradeoff, denoted by the area under the ROC curve (or AUC) is reduced for
545 Hispanics in both the datasets.
546

Taxon Associations

Taxon differential abundance across categorical metadata groups was performed in QIIME (QIIME: group_significance.py, **S5 Table**) to examine whether observation counts (i.e. OTUs and microbial taxon) are significantly different between groups within a metadata category (i.e. ethnicity, sex, BMI, age). The OTU table prior to final community quality control was collapsed at each taxonomic level (i.e. Phylum – Genus; QIIME: collapse_taxonomy.py), with counts representing the relative abundance of each microbial taxon. Differences in the mean abundance of taxa between ethnicities were calculated using Kruskal-Wallis nonparametric statistical tests. P-values are provided alongside false discovery rate and Bonferroni corrected P-values, and taxon were ranked from most to least significant. Results were collated into excel tables by taxonomic level and metadata category being examined, with significant (false discovery rate and Bonferroni P-value < 0.05) highlighted in orange, and taxa that were false discovery rate significant in both datasets were colored red. The Fisher's exact test for the overlap of number of significant taxa between datasets was run at the online portal (http://vassarstats.net/tab2x2.html), with the expected overlap calculated as 5% of the number of significant lineages at all taxonomic level within the respective dataset, and the observed 25 taxa that overlapped in our analysis. The permutation analysis was performed by comparing the number of significant taxa (**S5 Table**, $p_{FDR}<0.05$) overlapping between the AGP and HMP to the number overlapping when the Kruskal-Wallis test was performed 1,000 times with ethnicity randomly permuted. In 1/1000 runs there was one significant taxon overlapping at the family level, and one in 3/1000 permutations at the genus level, with no significant taxa overlapping in any repetitions at higher taxonomic levels. The 12 families and genera that were significantly different were evaluated to not be

570 'unique' if their abundances across ethnicities at each level represented at least 82-100%
571 (nearly all >95%) of the overlapping taxonomic level, and the genera was used if classified,
572 and family level used if genera was unclassified (g__). Average relative abundances on a log10
573 scale among individuals possessing the taxon were extracted for each taxon within each
574 ethnicity, and the abundance for 12 families and genera were made into barchart figures (**Fig**
575 **4**). The external whisker (AGP above, HMP below) depict the 75th quartile of abundance, and
576 the internal whisker depicts the 25th quartile. Pairwise Mann-Whitney-U tests were
577 performed between each pair of ethnicities using microbial abundances among all
578 individuals, and were Bonferroni corrected for the six comparisons within each taxon and
579 dataset. Bonferroni significant P-values are shown in the figure, and shown in bold if
580 significance and direction of change replicate in both datasets. Ubiquity shown above or
581 below each bar was calculated as the number of individuals in which that taxon was detected
582 within the respective ethnicity. Additional confirmation of ethnically varying abundance was
583 also performed at each taxonomic level (**S6 Table**), where the correlation of continuous age
584 and BMI along with categorically coded sex and ethnicity were simultaneously measured
585 against the log 10 transformed relative abundance of each taxon among individuals
586 possessing it using linear regression (**S6 Table** - Abundance), and against the presence or
587 absence of the taxon in all individuals with logistic regression (**S6 Table** - Presence Absence).
588 Significance is presented for the models each with ethnicity alone, and with all metadata
589 factors included (age, sex, BMI), alongside Bonferroni corrected p-values, and individual
590 effects of each metadata factor.
591
592 Co-Occurrence Analysis

Bacterial taxonomy was collapsed at the family level, Spearman correlation was calculated between each pair of families using SciPy (80), and clustermaps were generated using seaborn (**S2 Fig**), and ethnic associations were drawn from **S5 Table**. Correlations were masked where Bonferroni corrected Spearman p-values were >0.05, and clusters were identified as the most prominent (strongest correlations) and abundance enriched. Enrichment of ethnic association was evaluated by measuring the Mann-Whitney-U of cluster families ethnic associations (p-values, **S5 Table**) compared to the ethnic associations of non-cluster taxa. Cluster associated families were identified as having at least three significant correlations with families within the cluster.

Christensenellaceae Analysis

The abundance of the family Christensenellaceae was input as relative abundance across all individuals from the family level taxonomic table. Individuals were subset based on the presence/absence of Christensenellaceae and BMIs were compared using a one tailed Mann-Whitney-U test, then each was further subset by ethnicity and BMI compared using one tailed Mann-Whitney-U tests and boxplots within each ethnicity (**Fig 5**).

Genetically Associated, Heritable, and Correlated Taxa Analysis

Genetically associated taxa from population heritability studies (30, 31, 35, 36) with a minimum heritability (A in ACE models or H2r) >0.1, and from GWAS studies (31, 36) were examined for exact taxonomic overlap with our 12 ethnically-associated taxa. The 42 genetic variants associated with Unclassified Clostridiales are: rs16845116, rs586749, rs7527642, rs10221827, rs5754822, rs4968435, rs17170765, rs1760889, rs6933411, rs2830259,

rs7318523, rs17763551, rs2248020, rs1278911, rs185902, rs2505338, rs6999713, rs5997791, rs7236263, rs10484857, rs9938742, rs1125819, rs4699323, rs641527, rs7302174, rs2007084, rs2293702, rs9350764, rs2170226, rs2273623, rs9321334, rs6542797, rs9397927, rs2269706, rs4717021, rs7499858, rs10148020, rs7524581, rs11733214, rs7587067 from (31). These 40 variants along with variants in **Table 1** except for chr7:96414393 (total=49) were then assessed in 1,000 Genomes individuals for significant differentiation across superpopulations (34). The 1,000 Genomes VCF files were downloaded (ftp://ftp.1000genomes.ebi.ac.uk/vol1/ftp/release/20130502/), and variants with a minor allele frequency less than 0.01 were removed with F_{ST} calculated between each pair of superpopulations using vcftools (81). The East Asian versus South Asian F_{ST} rates were not used in the analysis. A custom script was used to examine the F_{ST} for each of the 49 variants and compare to the F_{ST} of all variants on the same chromosome and all variants genome-wide for that pair of populations, with percentile calculated and the number of variants with a higher F_{ST} divided by the total number of variants. The eQTL value and significance for rs7587067 were drawn from the GTEx database (67).

Data and Code Availability

Code, scripts, and data underlying figures are publicly available from the GitHub repository [https://github.com/awbrooks19/microbiota_and_ethnicity]. Individual metadata (age, sex, ethnicity…) for the Human Microbiome Project are held under restricted access available through dbGaP application [NCBI - dbGaP, Human Microbiome Project, https://www.ncbi.nlm.nih.gov/projects/gap/cgi-bin/study.cgi?study_id=phs000228.v3.p1].

Acknowledgements

This work was supported by National Institutes of Health training grants 4T32GM08017810, 5T32GM08017809, and 5T32GM0817808 to AWB, the Vanderbilt Office of Equity, Diversity and Inclusion to A.W.B. and S.R.B., the Vanderbilt Microbiome Initiative to S.R.B., and the Alfred P. Sloan Foundation Fellowship to R.B.. The content is solely the responsibility of the authors and does not necessarily represent the official views of the National Institutes of Health. We thank the American Society of Microbiology for supporting travel to present this work. We would also like to thank Tony Capra, David Samuels, Patrick Abbot, Antonis Rokas, and other members of the Vanderbilt Genetics Institute and Bordenstein Lab for input. The authors acknowledge the Minnesota Supercomputing Institute (MSI) at the University of Minnesota and the Advanced Computing Center for Research and Education (ACCRE) at Vanderbilt University for providing resources that contributed to the research results reported within this paper.

Contributions

A.W.B., S.P., R.B., and S.R.B. conceived and designed the research. A.W.B. performed, analyzed, and interpreted all experiments with the exception of the Random Forest analysis planned and performed by S.P. and R.B. S.R.B. supervised all experimental designs, data analysis, and data interpretation. All authors participated in manuscript preparation, editing, and final approval.

Competing Financial Interests

662 The authors declare no competing financial interests.

663

664

665 **Supplementary Table/Figure Legends:**

666 **S1 Fig.** The average relative abundance of dominant microbial phyla for each ethnicity.

667

668 **S2 Fig. Abundance correlation of microbial families.** Spearman correlation clustermaps
669 of bacterial abundance for families in the AGP and HMP. Numbers within boxes depict the
670 spearman correlation value with heatmap coloration from blue negative correlation (-1),
671 white no correlation (0), to red positive correlation (1). Positions have been masked based
672 on Bonferroni significance <0.05 for the total clustermap of all microbial families. Lineages
673 within boxes were identified as a highly correlated cluster, and lineages outside the boxes
674 share multiple correlations with those within the cluster. Blue taxonomic names indicate
675 overlap of taxa within boxes of both the AGP and HMP, while black indicate multiple
676 correlations with the clusters in both datasets. The ethnic association column depicts FDR
677 corrected p-values from Kruskal-Wallis tests in **S5 Table**, which are bolded if <0.05.

678

679 **S3 Fig. Correlation of BMI with Christensenellaceae abundance.** The relationship for
680 each individual between log10 transformed Christensenellaceae abundance on the y axis and
681 BMI on the x axis, with statistics slope, R^2, and p fit with a linear regression. Coloration of
682 each point indicates ethnicity: Yellow – African American; Blue – Asian-Pacific Islander;
683 Green – Hispanic; Red – Caucasian.

684

685 **S1 Table. Demographic information for the AGP.** Breakdown of age and BMI by sex and
686 ethnicity. Heatmaps were constructed within each statistic and category (bounded by black
687 box). The means for all sex and ethnic groups were used as the center (white), with higher

values indicated in red and lower in blue. HMP data is not shown because of data access restrictions on participant metadata, available through dbGaP application.

S2 Table. Microbiota distinguishability by ethnicity, age, sex and BMI. (A) AGP and HMP ANOSIM distinguishability by ethnicity, age, sex, and BMI at a rarefaction depth of 1,000 and across four ecological metrics (more details in table). (B) AGP ANOSIM distinguishability by ethnicity, age, sex, and BMI at rarefaction depths of 1,000 and 10,000. (C) ANOSIM results for consensus distance matrix while subsampling the maximum number of individuals from each ethnic group. (D) BioEnv results of correlation between ethnicity, age, sex, and BMI together with outcome as multivariate beta diversity distance matrices [Distance Matrix = Ethnicity*x1 + Categorical Age*x2 + Categorical BMI*x3 + Sex*x4 + B]. (E) ANOSIM results for consensus distance matrix when each ethnicity and group of ethnicities are sequentially removed from the analysis.

S3 Table. Alpha diversity by ethnicity, age, sex and BMI. Alpha Diversity for Ethnicity, Age, Sex, and BMI across varying rarefaction depths and beta diversity metrics in AG (4A, 4C-E), and for ethnicity in the HMP (4B). Results are based on non-parametric permutation based t-tests, and p-values are Bonferroni corrected within each factor of interest, depth, and metric.

S4 Table. Comparison of beta diversity distances for within and between ethnicities. All values depicted are Mann-Whitney-U p-values. (A) All distances between pairs of individuals within each ethnicity were compared between ethnicities across rarefaction

711 depths 1,000 and 10,000, four beta diversity metrics, and with while subsampling over-
712 represented ethnicities. (B) All distances between pairs of individuals within and between
713 each ethnicity were compared between ethnicities. (C) Mean distances between pairs of
714 individuals within each ethnicity were compared between ethnicities. (D) Mean distances
715 between pairs of individuals within and between each ethnicity were compared between
716 ethnicities.

717

718 **S5 Table. Taxa which are differentially abundant by ethnicity, sex, BMI, and age in the**
719 **AGP and HMP.** Kruskal-Wallis results for differential taxa abundance across metadata
720 groupings, including FDR and Bonferroni corrected p-values, and taxa abundance averages
721 within each group. Metadata factors and taxonomic levels are separated by excel tabs.

722

723 **S6 Table. Taxa which are correlated with ethnicity, sex, BMI, and age in the AGP.**
724 Results of linear (Abundance) and logistic (Presence Absence) regression results for
725 differential taxa abundance across metadata factors separated by taxonomic level. Columns
726 in order indicate the taxon name, the number of individuals with non-zero abundance; then
727 the p-value for ethnicity alone, the p-value Bonferroni corrected, the f-test statistic, and R^2;
728 then the same values for the regression with ethnicity, age, sex, and BMI together; then the
729 abundances in each ethnic group, and finally the p-values for each factor broken down.

730

731 **S7 Table. Genetic variants with taxa associations and detailed 1,000 Genomes**
732 **population differentiation rates (F_{ST}).** Variants in red indicate the variant has at least one
733 F_{ST} above the 95th percentile for high differentiation between at least one pair of populations.

Columns I-BU represent the values for calculating variant F_{ST} and percentiles. The first two spaces indicate the two superpopulations being compared. F_{ST} indicates the rate of differentiation for that variant between that pair of populations. Higher indicates the number of variants genome-wide with a higher F_{ST}, and total indicates the total genome-wide variants examined. The columns with chromosome indicate the number of variants with higher F_{ST} and total variants on the same chromosome as the variant of interest. Percent indicates the number of variants with a higher F_{ST} divided by the total number of variants.

References:

1. Turnbaugh PJ, Hamady M, Yatsunenko T, Cantarel BL, Duncan A, Ley RE, et al. A core gut microbiome in obese and lean twins. Nature. 2009;457(7228):480-4.
2. Qin J, Li R, Raes J, Arumugam M, Burgdorf KS, Manichanh C, et al. A human gut microbial gene catalogue established by metagenomic sequencing. Nature. 2010;464(7285):59-65.
3. Huse SM, Ye Y, Zhou Y, Fodor AA. A core human microbiome as viewed through 16S rRNA sequence clusters. PLoS One. 2012;7(6):e34242.
4. Wu GD, Chen J, Hoffmann C, Bittinger K, Chen YY, Keilbaugh SA, et al. Linking long-term dietary patterns with gut microbial enterotypes. Science. 2011;334(6052):105-8.
5. Muegge BD, Kuczynski J, Knights D, Clemente JC, González A, Fontana L, et al. Diet drives convergence in gut microbiome functions across mammalian phylogeny and within humans. Science. 2011;332:970-4.
6. Human Microbiome Project C. Structure, function and diversity of the healthy human microbiome. Nature. 2012;486(7402):207-14.
7. David LA, Maurice CF, Carmody RN, Gootenberg DB, Button JE, Wolfe BE, et al. Diet rapidly and reproducibly alters the human gut microbiome. Nature. 2013;505(7484):559-63.
8. Yatsunenko T, Rey FE, Manary MJ, Trehan I, Dominguez-Bello MG, Contreras M, et al. Human gut microbiome viewed across age and geography. Nature. 2012;486(7402):222-7.
9. Davenport ER, Cusanovich DA, Michelini K, Barreiro LB, Ober C, Gilad Y. Genome-Wide Association Studies of the Human Gut Microbiota. PLoS One. 2015;10(11):e0140301.
10. Fierera N, Hamadyc M, Lauberb CL, Knight R. The influence of sex, handedness, and washing on the diversity of hand surface bacteria. Procedings of the National Academy of Sciences.105(46).
11. Qin J, Li Y, Cai Z, Li S, Zhu J, Zhang F, et al. A metagenome-wide association study of gut microbiota in type 2 diabetes. Nature. 2012;490(7418):55-60.

12. Frank DN, Allison AL, Feldman RA, Boedeker EC, Harpaz N, Pace NR. Molecular-phylogenetic characterization of microbial community imbalances in human inflammatory bowel diseases. Procedings of the National Academy of Sciences. 2007(104):13780–5.
13. Walters WA, Xu Z, Knight R. Meta-analyses of human gut microbes associated with obesity and IBD. FEBS Lett. 2014;588(22):4223-33.
14. Zackular JP, Baxter NT, Iverson KD, Sadler WD, Petrosino JF, Chen GY, et al. The gut microbiome modulates colon tumorigenesis. MBio. 2013;4(6):e00692-13.
15. Mason MR, Nagaraja HN, Camerlengo T, Joshi V, Kumar PS. Deep sequencing identifies ethnicity-specific bacterial signatures in the oral microbiome. PLoS One. 2013;8(10):e77287.
16. Ravela J, Gajera P, Abdob ZG, Schneiderc M, Koeniga SSK, McCullea SL, et al. Vaginal microbiome of reproductive-age women. Procedings of the National Academy of Sciences. 2011;108:4680-7.
17. Fettweis JM, Brooks JP, Serrano MG, Sheth NU, Girerd PH, Edwards DJ, et al. Differences in vaginal microbiome in African American women versus women of European ancestry. Microbiology. 2014;160(Pt 10):2272-82.
18. Williams DR, Priest N, Anderson NB. Understanding associations among race, socioeconomic status, and health: Patterns and prospects. Health Psychol. 2016;35(4):407-11.
19. Mersha TB, Abebe T. Self-reported race/ethnicity in the age of genomic research: its potential impact on understanding health disparities. Human Genomics. 2015;9(1):1.
20. McDonald D, Birmingham A, Knight R. Context and the human microbiome. Microbiome. 2015;3:52.
21. Kolde R, Franzosa EA, Rahnavard G, Hall AB, Vlamakis H, Stevens C, et al. Host genetic variation and its microbiome interactions within the Human Microbiome Project. Genome Med. 2018;10(1):6.
22. Rothschild D, Weissbrod O, Barkan E, Korem T, Zeevi D, Costea PI, et al. Environmental factors dominate over host genetics in shaping human gut microbiota composition. BioRxiv. 2017.
23. DeSantis TZ, Hugenholtz P, Larsen N, Rojas M, Brodie EL, Keller K, et al. Greengenes, a chimera-checked 16S rRNA gene database and workbench compatible with ARB. Appl Environ Microbiol. 2006;72(7):5069-72.
24. Clarke KR. Non-parametric multivariate analyses of changes in community structure. Australian Journal of Ecology. 1993;18:117-43.
25. Clarke KR, Ainsworth M. A method of linking multivariate community structure to environmental variables. Marine Ecology. 1993;92:205-19
.
26. Knights D, Costello EK, Knight R. Supervised classification of human microbiota. FEMS Microbiol Rev. 2011;35(2):343-59.
27. Shannon CE. A mathematical theory of communication. Bell Syst Tech J. 1948;27:379-423.
28. Hester ER, Barott KL, Nulton J, Vermeij MJ, Rohwer FL. Stable and sporadic symbiotic communities of coral and algal holobionts. ISME J. 2016;10(5):1157-69.
29. N.V. C, K.W. B, L.O. H, W.P. K. SMOTE: Synthetic Minority Over-sampling Technique. Journal of Artificial Intelligence Research. 2002;16:321-57.

814 30. Goodrich JK, Waters JL, Poole AC, Sutter JL, Koren O, Blekhman R, et al. Human
815 genetics shape the gut microbiome. Cell. 2014;159(4):789-99.
816 31. Goodrich JK, Davenport ER, Beaumont M, Jackson MA, Knight R, Ober C, et al. Genetic
817 Determinants of the Gut Microbiome in UK Twins. Cell Host Microbe. 2016;19(5):731-43.
818 32. Fu J, Bonder MJ, Cenit MC, Tigchelaar EF, Maatman A, Dekens JA, et al. The Gut
819 Microbiome Contributes to a Substantial Proportion of the Variation in Blood Lipids. Circ
820 Res. 2015;117(9):817-24.
821 33. Pennisi E. Human Genetic Variation. Science. 2007;318(5858):1842-3.
822 34. Genomes Project C, Auton A, Brooks LD, Durbin RM, Garrison EP, Kang HM, et al. A
823 global reference for human genetic variation. Nature. 2015;526(7571):68-74.
824 35. Lim MY, You HJ, Yoon HS, Kwon B, Lee JY, Lee S, et al. The effect of heritability and
825 host genetics on the gut microbiota and metabolic syndrome. Gut. 2016.
826 36. Turpin W, Espin-Garcia O, Xu W, Silverberg MS, Kevans D, Smith MI, et al.
827 Association of host genome with intestinal microbial composition in a large healthy cohort.
828 Nature Genetics. 2016;48(11):1413-7.
829 37. Almasy L, Blangero J. Multipoint quantitative-trait linkage analysis in general
830 pedigrees. Am J Hum Genet. 1998;62(5):1198-211.
831 38. Morgan XC, Tickle TL, Sokol H, Gevers D, Huttenhower C. Dysfunction of the
832 intestinal microbiome in inflammatory bowel disease and treatment. Genome Biology.
833 2012;7(979).
834 39. Lewis JD, Chen EZ, Baldassano RN, Otley AR, Griffiths AM, Lee D, et al. Inflammation,
835 Antibiotics, and Diet as Environmental Stressors of the Gut Microbiome in Pediatric Crohn's
836 Disease. Cell Host Microbe. 2015;18(4):489-500.
837 40. Goker M, Gronow S, Zeytun A, Nolan M, Lucas S, Lapidus A, et al. Complete genome
838 sequence of Odoribacter splanchnicus type strain (1651/6). Stand Genomic Sci.
839 2011;4(2):200-9.
840 41. Castaneda G, Liu B, Torres S, Bhuket T, Wong RJ. Race/Ethnicity-Specific Disparities
841 in the Severity of Disease at Presentation in Adults with Ulcerative Colitis: A Cross-
842 Sectional Study. Dig Dis Sci. 2017.
843 42. Boucias DG, Cai Y, Sun Y, Lietze VU, Sen R, Raychoudhury R, et al. The hindgut lumen
844 prokaryotic microbiota of the termite Reticulitermes flavipes and its responses to dietary
845 lignocellulose composition. Mol Ecol. 2013;22(7):1836-53.
846 43. LATHAM MJ, WOLIN MJ. Fermentation of Cellulose by Ruminococcus flavefaciens in
847 the Presence and Absence ofMethanobacterium ruminantium. Appl Environ Microbiol.
848 1977;34(3):297-301.
849 44. Falony G, Raes J. Population-level analysis of gut microbiome variation. Science.
850 2016;352(6285):560-4.
851 45. Biagi E, Franceschi C, Rampelli S, Severgnini M, Ostan R, Turroni S, et al. Gut
852 Microbiota and Extreme Longevity. Curr Biol. 2016;26(11):1480-5.
853 46. Thevaranjan N, Puchta A, Schulz C, Naidoo A, Szamosi JC, Verschoor CP, et al. Age-
854 Associated Microbial Dysbiosis Promotes Intestinal Permeability, Systemic Inflammation,
855 and Macrophage Dysfunction. Cell Host Microbe. 2017;21(4):455-66 e4.
856 47. Xie W, Wood AR, Lyssenko V, al. e. Genetic Variants Associated With Glycine
857 Metabolism and Their Role in Insulin Sensitivity and Type 2 Diabetes. Diabetes. 2013;62.
858 48. Williams SR, Yang Q, Chen F, Liu X, Keene KL, Jacques P, et al. Genome-wide meta-
859 analysis of homocysteine and methionine metabolism identifies five one carbon

metabolism loci and a novel association of ALDH1L1 with ischemic stroke. PLoS Genet. 2014;10(3):e1004214.
49. Petersen LM, Bautista EJ, Nguyen H, Hanson BM, Chen L, Lek SH, et al. Community characteristics of the gut microbiomes of competitive cyclists. Microbiome. 2017;5(1):98.
50. Nakamura N, Lin HC, McSweeney CS, Mackie RI, Gaskins HR. Mechanisms of microbial hydrogen disposal in the human colon and implications for health and disease. Annu Rev Food Sci Technol. 2010;1:363-95.
51. Parthasarathy G, Chen J, Chen X, Chia N, O'Connor HM, Wolf PG, et al. Relationship Between Microbiota of the Colonic Mucosa vs Feces and Symptoms, Colonic Transit, and Methane Production in Female Patients With Chronic Constipation. Gastroenterology. 2016;150(2):367-79 e1.
52. Jackson CS, Oman M, Patel AM, Vega KJ. Health disparities in colorectal cancer among racial and ethnic minorities in the United States. J Gastrointest Oncol. 2016;7:S32-43.
53. Lopetuso LR, Scaldaferri F, Petito V, Gasbarrini A. Commensal Clostridia: leading players in the maintenance of gut homeostasis. Gut Pathogens. 2013.
54. Sy DF. The Center for Asian Health Engages Communities in Research to Reduce Asian American Health Disparities. US Department of Health & Human Services, National Institute on Minority Health and Health Disparities.
55. Hwang H. Colorectal Cancer Screening among Asian Americans. Asian Pacific Journal of Cancer Prevention. 2013;14(7):4025-32.
56. Oh KM, Kreps GL, Jun J. Colorectal Cancer Screening Knowledge, Beliefs, and Practices of Korean Americans. American Journal of Health Behavior. 2013;37(3):381-94.
57. Sankaranarayanan R, Ramadas K, Qiao Y-l. Managing the changing burden of cancer in Asia. BMC Medicine. 2014;12(3).
58. Pourhoseingholi MA. Increased burden of colorectal cancer in Asia. World J Gastrointest Oncol. 2012;4(4):68-70.
59. Pourhoseingholi MA, Vahedi M, Baghestani AR. Burden of gastrointestinal cancer in Asia; an overview. Gastroenterology and Hepatology. 2015.
60. Pourhoseingholi MA. Epidemiology and burden of colorectal cancer in Asia-Pacific region: what shall we do now? Translational Gastrointestinal Cancer. 2014;3(4):169-73.
61. Report CHDaI. 2013.
62. Cao H, Liu X, An Y, Zhou G, Liu Y, Xu M, et al. Dysbiosis contributes to chronic constipation development via regulation of serotonin transporter in the intestine. Sci Rep. 2017;7(1):10322.
63. Mosca A, Leclerc M, Hugot JP. Gut Microbiota Diversity and Human Diseases: Should We Reintroduce Key Predators in Our Ecosystem? Front Microbiol. 2016;7:455.
64. Zhang X, Zhang D, Jia H, Feng Q, Wang D, Liang D, et al. The oral and gut microbiomes are perturbed in rheumatoid arthritis and partly normalized after treatment. Nat Med. 2015;21(8):895-905.
65. Singh VP, Proctor SD, Willing BP. Koch's postulates, microbial dysbiosis and inflammatory bowel disease. Clin Microbiol Infect. 2016;22(7):594-9.
66. Sherry ST WM, Kholodov M, Baker J, Phan L, Smigielski EM, Sirotkin K. dbSNP: the NCBI database of genetic variation. Nucleic Acids Research. 2001;29(308).
67. Consortium GT. The Genotype-Tissue Expression (GTEx) project. Nat Genet. 2013;45(6):580-5.

906 68. Qiu X, Wei R, Li Y, Zhu Q, Xiong C, Chen Y, et al. NEDL2 regulates enteric nervous
907 system and kidney development in its Nedd8 ligase activity-dependent manner.
908 Oncotarget. 2016;7(21).
909 69. Wei R, Qiu X, Wang S, Li Y, Wang Y, Lu K, et al. NEDL2 is an essential regulator of
910 enteric neural development and GDNF/Ret signaling. Cell Signal. 2015;27(3):578-86.
911 70. O'Donnell AM, Coyle D, Puri P. Decreased expression of NEDL2 in Hirschsprung's
912 disease. J Pediatr Surg. 2016;51(11):1839-42.
913 71. Roberts SJ, Stewart AJ, Schmid R, Blindauer CA, Bond SR, Sadler PJ, et al. Probing the
914 substrate specificities of human PHOSPHO1 and PHOSPHO2. Biochim Biophys Acta.
915 2005;1752(1):73-82.
916 72. Ikeda M, Hosotani T, Kurimoto K, Mori T, Ueda T, Kotake Y, et al. The differences of
917 the metabolism related to vitamin B6-dependent enzymes among vitamin B6-deficient
918 germ-free and conventional rats. Nutritional Science Vitaminology. 1979;131(9).
919 73. Nagy-Szakal D, Williams BL, Mishra N, Che X, Lee B, Bateman L, et al. Fecal
920 metagenomic profiles in subgroups of patients with myalgic encephalomyelitis/chronic
921 fatigue syndrome. Microbiome. 2017;5(1):44.
922 74. Bhui KS, Dinos S, Ashby D, Nazroo J, Wessely S, White PD. Chronic fatigue syndrome
923 in an ethnically diverse population: the influence of psychosocial adversity and physical
924 inactivity. BMC Medicine. 2011;9(26).
925 75. Caporaso JG, Kuczynski J, Stombaugh J, Bittinger K, Bushman FD, Costello EK, et al.
926 QIIME allows analysis of high-throughput community sequencing data. Nat Method.
927 2010;7:335-6.
928 76. Caporaso JG, Lauber CL, Walters WA, Berg-Lyons D, Huntley J, Fierer N, et al. Ultra-
929 high-throughput microbial community analysis on the Illumina HiSeq and MiSeq platforms.
930 ISME J. 2012;6(8):1621-4.
931 77. Anderson MJ. A new method for non-parametric multivariate analysis of variance.
932 Australian Journal of Ecology. 2001;26:32-46.
933 78. McMurdie PJ, Holmes S. phyloseq: an R package for reproducible interactive analysis
934 and graphics of microbiome census data. PLoS One. 2013;8:e61217.
935 79. Kuhn M. A short introduction to the caret package. 2017.
936 80. Jones E, Oliphant T, Peterson P. Open Source Scientific Tools for Python. 2001.
937 81. Danecek P, Auton A, Abecasis G, Albers CA, Banks E, DePristo MA, et al. The variant
938 call format and VCFtools. Bioinformatics. 2011;27(15):2156-8.

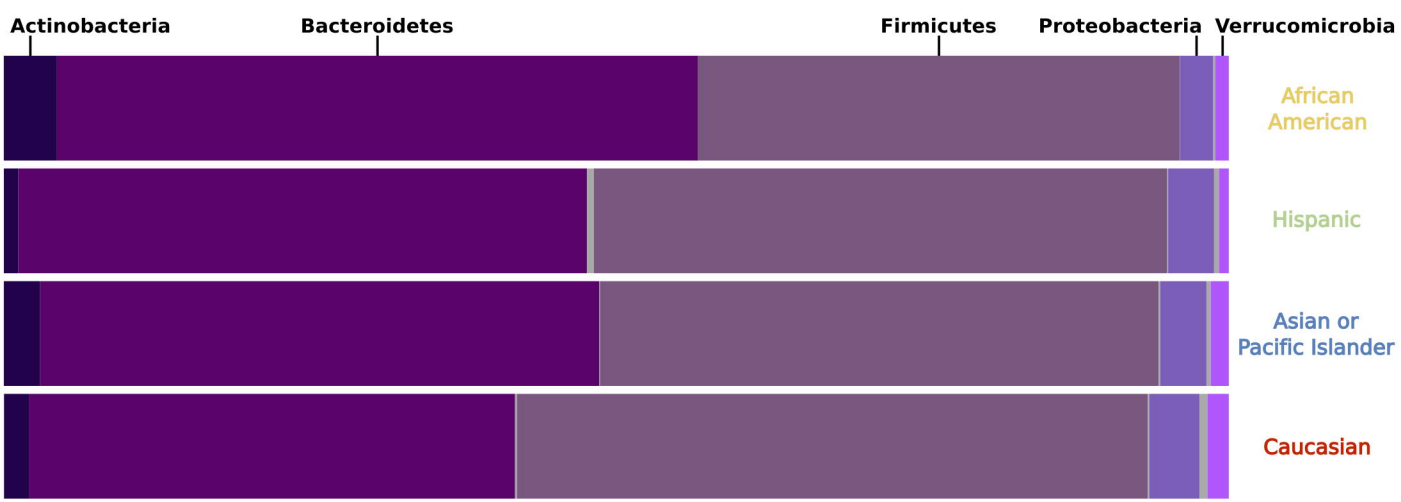
Actinobacteria
Bacteroidetes
Firmicutes
Proteobacteria
Verrucomicrobia
African American
Hispanic
Asian or Pacific Islander
Caucasian

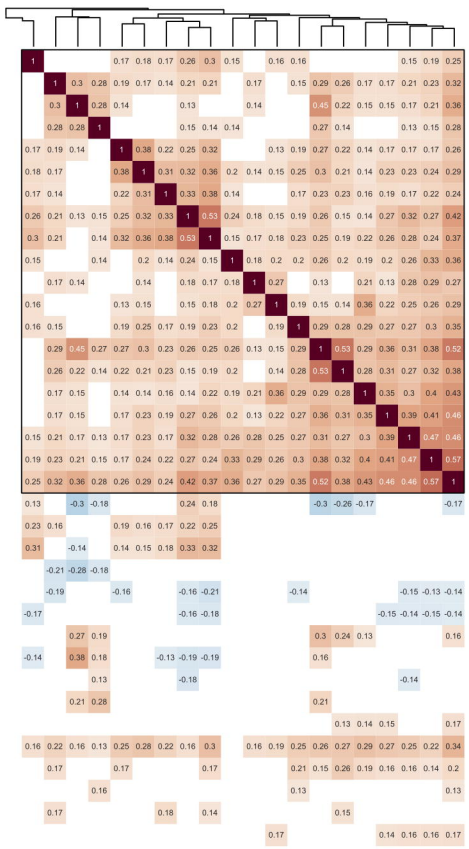

Taxonomic Lineage (Blue: Overlap Within Cluster | Bold: Overlap Correlated with Cluster)	Ethnic Association (Bold: FDR Significant p-value)
k__Bacteria; p__Proteobacteria; c__Deltaproteobacteria; o__Desulfovibrionales; f__Desulfovibrionaceae	**0.00067**
k__Bacteria; p__Firmicutes; c__Clostridia; o__Clostridiales; f__Peptococcaceae	**0.00138**
k__Bacteria; p__Firmicutes; c__Clostridia; o__Clostridiales; f__Ruminococcaceae	**0.00085**
k__Bacteria; p__Firmicutes; c__Clostridia; o__Clostridiales; f__[Mogibacteriaceae]	**0.00171**
k__Bacteria; p__Cyanobacteria; c__4C0d-2; o__YS2; f__	**3.38e-6**
k__Bacteria; p__Proteobacteria; c__Alphaproteobacteria; o__RF32; f__	**4.10e-6**
k__Bacteria; p__Bacteroidetes; c__Bacteroidia; o__Bacteroidales; f__[Barnesiellaceae]	**0.00606**
k__Bacteria; p__Bacteroidetes; c__Bacteroidia; o__Bacteroidales; f__Rikenellaceae	**7.36e-6**
k__Bacteria; p__Bacteroidetes; c__Bacteroidia; o__Bacteroidales; f__[Odoribacteraceae]	**0.00087**
k__Bacteria; p__Verrucomicrobia; c__Verrucomicrobiae; o__Verrucomicrobiales; f__Verrucomicrobiaceae	**3.93e-6**
k__Bacteria; p__Firmicutes; c__Clostridia; o__Clostridiales; f__EtOH8	0.60348
k__Bacteria; p__Synergistetes; c__Synergistia; o__Synergistales; f__Synergistaceae	0.24561
k__Bacteria; p__Proteobacteria; c__Betaproteobacteria; o__Burkholderiales; f__Oxalobacteraceae	**0.01552**
k__Bacteria; p__Firmicutes; c__Clostridia; o__Clostridiales; f__	**9.29e-9**
k__Bacteria; p__Tenericutes; c__Mollicutes; o__RF39; f__	**0.00281**
k__Archaea; p__Euryarchaeota; c__Methanobacteria; o__Methanobacteriales; f__Methanobacteriaceae	**0.00142**
k__Bacteria; p__Tenericutes; c__RF3; o__ML615J-28; f__	**0.00517**
k__Bacteria; p__Firmicutes; c__Clostridia; o__SHA-98; f__	**0.00342**
k__Bacteria; p__Firmicutes; c__Clostridia; o__Clostridiales; f__Dehalobacteriaceae	**0.00336**
k__Bacteria; p__Firmicutes; c__Clostridia; o__Clostridiales; f__Christensenellaceae	**1.55e-9**
k__Bacteria; p__Bacteroidetes; c__Bacteroidia; o__Bacteroidales; f__Bacteroidaceae	0.65799
k__Bacteria; p__Proteobacteria; c__Betaproteobacteria; o__Burkholderiales; f__Alcaligenaceae	0.38689
k__Bacteria; p__Bacteroidetes; c__Bacteroidia; o__Bacteroidales; f__Porphyromonadaceae	**0.00517**
k__Bacteria; p__Proteobacteria; c__Gammaproteobacteria; o__Enterobacteriales; f__Enterobacteriaceae	0.24790
k__Bacteria; p__Actinobacteria; c__Actinobacteria; o__Bifidobacteriales; f__Bifidobacteriaceae	**2.11e-5**
k__Bacteria; p__Firmicutes; c__Bacilli; o__Lactobacillales; f__Streptococcaceae	0.64088
k__Bacteria; p__Firmicutes; c__Clostridia; o__Clostridiales; f__Clostridiaceae	0.64362
k__Bacteria; p__Firmicutes; c__Clostridia; o__Clostridiales; f__Lachnospiraceae	0.35217
k__Bacteria; p__Firmicutes; c__Erysipelotrichi; o__Erysipelotrichales; f__Erysipelotrichaceae	0.99041
k__Bacteria; p__Actinobacteria; c__Coriobacteriia; o__Coriobacteriales; f__Coriobacteriaceae	0.70082
k__Bacteria; p__Verrucomicrobia; c__Opitutae; o__[Cerasicoccales]; f__[Cerasicoccaceae]	0.99041
k__Bacteria; p__Lentisphaerae; c__[Lentisphaeria]; o__Victivallales; f__Victivallaceae	**0.00606**
k__Bacteria; p__Bacteroidetes; c__Bacteroidia; o__Bacteroidales; f__S24-7	0.38689
k__Bacteria; p__Bacteroidetes; c__Bacteroidia; o__Bacteroidales; f__Prevotellaceae	0.21918
k__Bacteria; p__Bacteroidetes; c__Bacteroidia; o__Bacteroidales; f__[Paraprevotellaceae]	0.96330
k__Archaea; p__Euryarchaeota; c__Thermoplasmata; o__E2; f__[Methanomassiliicoccaceae]	0.54235

American Gut Project

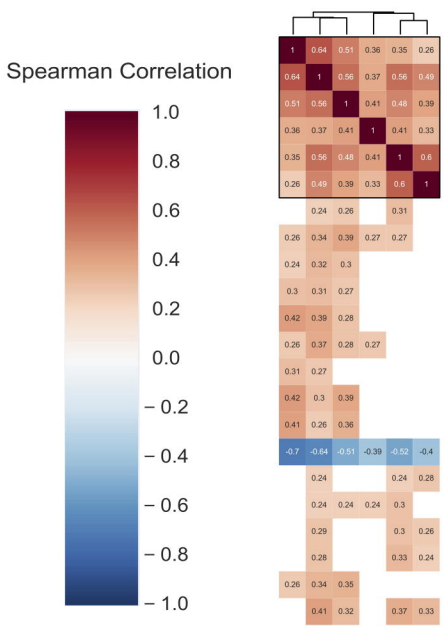

k__Bacteria; p__Firmicutes; c__Clostridia; o__Clostridiales; f__Ruminococcaceae	0.18789
k__Bacteria; p__Firmicutes; c__Clostridia; o__Clostridiales; f__	**0.00463**
k__Bacteria; p__Firmicutes; c__Clostridia; o__Clostridiales; f__Christensenellaceae	**0.00193**
k__Bacteria; p__Firmicutes; c__Clostridia; o__Clostridiales; f__Dehalobacteriaceae	**0.02336**
k__Bacteria; p__Tenericutes; c__Mollicutes; o__RF39; f__	**0.00718**
k__Bacteria; p__Tenericutes; c__RF3; o__ML615J-28; f__	0.08836
k__Bacteria; p__Bacteroidetes; c__Bacteroidia; o__Bacteroidales; f__Prevotellaceae	**0.03608**
k__Bacteria; p__Firmicutes; c__Clostridia; o__Clostridiales; f__Peptococcaceae	**0.02300**
k__Bacteria; p__Firmicutes; c__Erysipelotrichi; o__Erysipelotrichales; f__Erysipelotrichaceae	0.23592
k__Bacteria; p__Firmicutes; c__Clostridia; o__Clostridiales; f__Clostridiaceae	0.23592
k__Bacteria; p__Firmicutes; c__Clostridia; o__Clostridiales; f__Lachnospiraceae	0.31072
k__Bacteria; p__Verrucomicrobia; c__Verrucomicrobiae; o__Verrucomicrobiales; f__Verrucomicrobiaceae	**0.04723**
k__Bacteria; p__Firmicutes; c__Bacilli; o__Lactobacillales; f__Streptococcaceae	0.57953
k__Bacteria; p__Actinobacteria; c__Coriobacteriia; o__Coriobacteriales; f__Coriobacteriaceae	**0.00660**
k__Bacteria; p__Firmicutes; c__Clostridia; o__Clostridiales; f__[Mogibacteriaceae]	0.23592
k__Bacteria; p__Bacteroidetes; c__Bacteroidia; o__Bacteroidales; f__Bacteroidaceae	**0.00629**
k__Bacteria; p__Lentisphaerae; c__[Lentisphaeria]; o__Victivallales; f__Victivallaceae	**0.02558**
k__Bacteria; p__Proteobacteria; c__Betaproteobacteria; o__Burkholderiales; f__Oxalobacteraceae	0.18294
k__Bacteria; p__Firmicutes; c__Clostridia; o__SHA-98; f__	0.59964
k__Bacteria; p__Bacteroidetes; c__Bacteroidia; o__Bacteroidales; f__S24-7	0.11834
k__Bacteria; p__Bacteroidetes; c__Bacteroidia; o__Bacteroidales; f__Rikenellaceae	**0.00376**
k__Bacteria; p__Bacteroidetes; c__Bacteroidia; o__Bacteroidales; f__[Odoribacteraceae]	**0.00629**

Human Microbiome Project

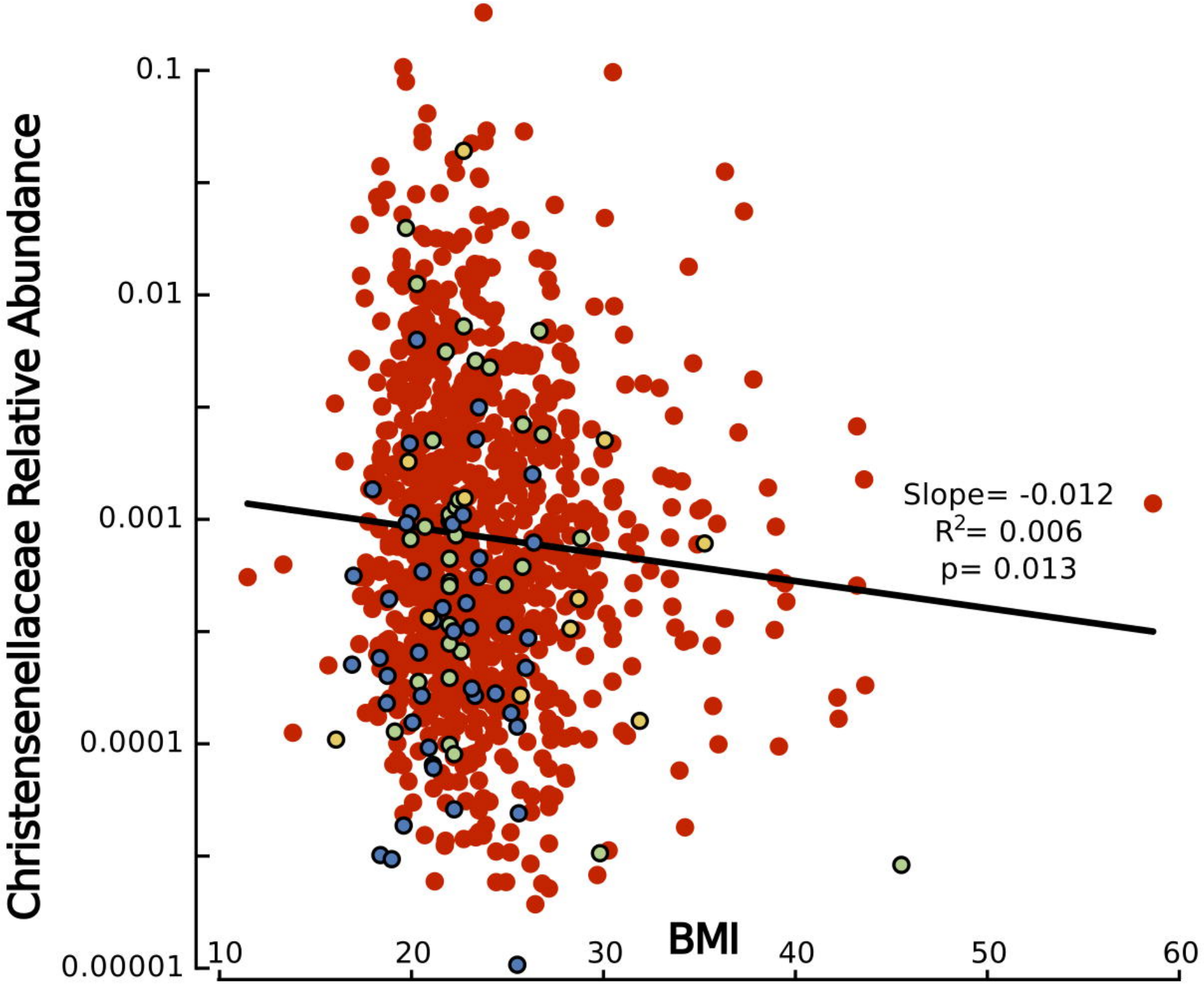
Christensenellaceae Relative Abundance
0.1
0.01
0.001
0.0001
0.00001
10
20
30
40
50
60
BMI
Slope= -0.012
R2= 0.006
p= 0.013